THE EFFECTS OF LIGAMENTOUS INJURY IN THE HUMAN LOWER CERVICAL SPINE

P Devin Leahy[1] and **Christian M Puttlitz**[1,2,3]

[1]Orthopaedic Bioengineering Research Laboratory, Department of Mechanical Engineering, Colorado State University, Fort Collins, CO 80523, USA

[2]School of Biomedical Engineering, Colorado State University, Fort Collins, CO 80523, USA

[3]Department of Clinical Sciences, Colorado State University, Fort Collins, CO 80523, USA

Abstract

Damage is often sustained by the anterior longitudinal ligament (ALL) and ligamentum flavum LF) in the cervical spine subsequent to whiplash or other cervical trauma. These ligaments afford substantial cervical stability when healthy, but the ability of the ALL and LF to stabilize the spine when injured is not as conclusively studied. In order to address this issue, the current study excised ALL and LF tissues from cadaveric spines and experimentally simulated whiplash-type damage to the isolated ligaments. Stiffnesses and toe region lengths were measured for both the uninjured and damaged states. These ligamentous mechanical properties were then inputted into a previously-validated finite element (FE) model of the cervical spine and the kinematic effects of various clinically relevant combinations of ligamentous injury were predicted. The data indicated three and five-fold increases in toe region length for the LF and ALL injury variants, respectively. These toe length distensions resulted in FE predictions of supra-physiologic ranges of motion, and these motions were comparable to spines with no ligamentous support. Finally, a set of cadaveric cervical spine ligament-sectioning experiments confirmed the FE predictions and supported the finding that partial injury to the relevant ligaments produces equivalent cervical kinematic signatures to spines that have completely compromised ALL and LF tissues.

Introduction

Cervical spine ligaments are frequently damaged during head impact and/or other cervical trauma, potentially leading to spinal instability (Ivancic et al., 2004; Panjabi et al., 2004). A common injury mechanism is whiplash, which is capable of damaging both the posterior and/or anterior ligamentous structures (Tominaga et al., 2006). Depending on the load application vector, whiplash injuries may involve cervical hyperextension and/or hyperflexion (Foreman and Croft, 2002). Hyperextension places the anterior longitudinal

Corresponding Author Christian Puttlitz, PhD, Monfort Professor, Director, Orthopaedic Bioengineering Research Laboratory, Associate Professor, Department of Mechanical Engineering, Associate Professor, School of Biomedical Engineering, Associate Professor, Department of Clinical Sciences, Colorado State University, 1374 Campus Delivery, Fort Collins, CO 80523-1374, Tel: 970.491.0956, puttlitz@engr.colostate.edu.

Conflict of Interest Statement

The authors have no conflicts of interest to disclose.

ligament (ALL) and facet capsule (FC) ligaments at risk, and hyperflexion motion often damages the flaval (LF) and interspinous ligaments (ISL) (Ivancic et al., 2004; Panjabi et al., 2004). Previous *in-vitro* whiplash simulations have measured the magnitude of ligamentous elongation during these loading events, and have also found total quasi-static cervical flexion and extension range of motion (ROM) after a simulated traumatic whiplash event to be supra-physiologic (Ito et al., 2004; Ivancic et al., 2004; Panjabi et al., 2004). However, these studies examined the cervical spine in its entirety, where it is difficult to discern the mechanical contribution of specific ligaments relative to auxiliary structural tissues (such as the intervertebral discs).

Maintaining proper cervical stability is critical, since supra-physiologic ROM can produce nervous tissue impingement and injuries to other peri-spinous soft tissues (White III and Panjabi, 1990; Ivancic et al., 2004; Hogan et al., 2005; Dickerman et al., 2006). It is unknown what capability the injured ligaments have in limiting cervical ROM below non-damaging levels. Thus, determining the mechanical properties of these injured ligaments is a vital step in understanding how to clinically treat and stabilize severe whiplash injuries, thereby minimizing the potential for permanent neural impairment (Dickman et al., 1991; Hogan et al., 2005; Panjabi et al., 2006).

In response, the goal of the current study was to measure the effect of post-traumatic damage on the mechanical properties of cervical ligaments, and model the kinematic alterations experienced by the cervical spine as a result of these specific ligamentous injuries. The initial aim was accomplished by excising individual ligaments from the cervical spine, wherein the intact (uninjured) and post-injury mechanical properties of these tissues could be consecutively measured. Testing of ligamentous properties focused on the ALL and LF. The ALL and LF ligaments were chosen as they: 1) have been found to greatly influence spinal mechanics; 2) have vastly different ratios of collagen to elastin content; and 3) are commonly injured from excessive strains experienced during whiplash-type trauma (Panjabi et al., 1975; Ivancic et al., 2004; Mow and Huiskes, 2005). Assessment of the effects of ligamentous injury on cervical flexibility was accomplished by inputting the measured ligamentous mechanical properties into finite element (FE) models of the cervical spine.

Materials and Methods

The methodology involved three phases: 1) physical experimentation on ligaments to determine the alterations in their mechanical properties due to damage; 2) FE predictions of the cervical kinematics that result from this ligamentous damage; and 3) cadaveric cervical spine experimentation to demonstrate the predictive accuracy of the FE model.

Ligament Damage Experimentation

Five male and two female cadaveric C0–C7 spines (average age: 53.1 years) were denuded of their musculature and other extraneous tissues with care taken to preserve the ligamentous structures. Bone-ligament-bone specimens were extracted from the spines with a diamond-bladed bandsaw (Exakt model 30/736, Exakt Apparetebau GmbH & Co., Norderstedt, Germany). The total yield of the 7 spines included 14 ALL (C2–C3: n = 6, C4–C5: n = 6, C5–C6: n = 1, C6–C7: n = 1) and 12 LF (C2–C3: n = 7, C4–C5: n = 4, C6–C7: n = 1) specimens. The bony portions of the specimens were potted in poly-methyl-methacrylate (PMMA). Self-tapping screws were inserted into the osseous tissues to increase purchase and reduce the possibility of slippage within the PMMA. Visual inspection of the bony tissues' position within the PMMA was made both before and after the testing procedure to ensure slippage did not occur.

Tensile testing of the individual ligaments was accomplished with a servo-hydraulic loadframe (Mini Bionix II, model 858, MTS, Eden Prairie, MN; Figure 1). Displacement was measured via a crosshead-mounted linear variable differential transformer (LVDT), and the associated force was measured by an inline load-cell (5 kN capacity, Model 661.19-01, MTS, Eden Prairie, MN). Specimens were housed within a heated, saline-filled tank which maintained physiologic temperature (37°C) and hydration. Reference position (displacement = 0 mm) was defined by the extension of the resting ligaments when weighted by the upper potting box (approximately 300 g) while submerged in saline. The loadframe actuator was lowered until a hole in the actuator fixture aligned with a hole in the upper potting box. A shear pin could only be inserted when the two components were vertically aligned within ±0.01 mm with no preload force, ensuring an equal starting position and tension for all ligaments. The lower potting box was mounted on a custom-made, biaxially-translating table to enable horizontal alignment. An automated testing sequence was developed that required no user intervention beyond zeroing the LVDT and load-cell at the beginning of the test. The testing sequence was accomplished using the following protocol: 1) increase displacement to induce a 5 N tensile load, hold displacement at this level for 10 minutes for tissue relaxation; 2) apply 120 cycles of sinusoidal displacement (0.0 to 0.4 mm relative to the displacement at the beginning of the step) at 1 Hz for preconditioning, and quasi-statically (0.2 mm/s) ramp from zero displacement to 40 N to determine initial stiffness; 3) dwell 10 minutes; 4) apply 120 cycles of sinusoidal displacement for preconditioning and quasi-statically ramp from zero displacement to 40 N for a duplicate initial stiffness measurement; 5) induce partial ligament damage (detailed below); 6) apply 120 cycles of sinusoidal displacement for preconditioning and quasi-statically ramp from zero displacement to 40 N to determine the final stiffness at 10, 30, and 90 minutes after the damage step. The 40 N maximum force was chosen as it tensioned the ligaments throughout the extension ranges typically experienced during normal, physiologic cervical motion (Womack et al., 2011).

The partial ligament damage protocol (Step 5) was executed by quasi-statically preloading the ligaments to 10 N to remove appreciable slack in the tissues and testing mechanism, rapidly tensioning the ligaments at 50 mm/s, and immediately reversing the actuator at 35 mm/s when the load-cell detected a specified drop in force that indicated initial tearing of the ligaments. Approximately 0.05 s were required to accelerate the actuator to 50 mm/s from the 0.2 mm/s rate immediately preceding damage. The force drop values were set to 1% for the ALL specimens and 3% for LF specimens. These magnitudes were determined from pilot experiments to consistently induce damage without completely compromising the ligaments. The loading rate was modeled after a strain rate of 10/s, which has been reported for impact trauma events (Lucas et al., 2008). Force and displacement data were recorded at 205 Hz for the quasi-static loads and 1024 Hz for the high-rate loads.

Stiffness values were calculated via linear regression of the force/displacement data at discrete force intervals: between 10–20 N, 20–30 N, and 30–40 N. The calculation of stiffness at discrete force intervals was undertaken to account for the permanent yield expected after inducing damage as well as to capture the nonlinear mechanical behavior typically observed in ligaments. Displacement at the 10 N (which defined the initial toe region length) and 40 N force levels were also compared before and after injury to quantify the amount of permanent distension due to the damage protocol. Percentage change values were calculated relative to the pre-damage state.

Statistical analyses were performed to determine significant differences between the stiffness and initial toe length readings for each of the five measurement timepoints specified in the testing protocol. A square root transformation was used to normalize the residuals, and therefore these values were independent of the means (SAS V9.2, Cary, NC).

Analyses were conducted with a randomized block design, blocking on ligament type (ALL or LF) and measurement time as a fixed effect. P-values less than 0.01 were considered significant.

Computational Modeling

A previously-developed C3–C7 FE model (ABAQUS V6.9-EF2, Dassault Systèmes Simulia Corp, Providence, RI) of the human cervical spine was modified to simulate the mechanical effects of hyperextension and hyperflexion injuries at the most common level of whiplash injury, C5–C6 (Ivancic et al., 2004). This model has been previously validated and converged for intact behavior (Womack et al., 2011). In brief, the anatomic geometry was generated from a single computed-tomography (CT) scan of an average-sized cadaveric spine. Validation was accomplished by pure-moment testing of cadaveric (C3–C7) osteoligamentous spines (n = 6) where intervertebral ROM, facet contact pressure, cortical strain in the lamina, nucleus pulposus pressure, and annulus fibrosus bulge were measured during quasi-static loadings. These loads consisted of ±2 Nm moments applied to the C3 vertebra in the axial rotation, lateral bending, and flexion and extension directions via a custom-designed, force-feedback robotic testing arm. C7 was rigidly fixed to a 6-degree of freedom load cell. Convergence was achieved by comparing the predicted values for the aforementioned validation parameters between four models of varied mesh resolution.

FE simulations of the hyperextension and hyperflexion injuries were conducted as both full and partial damage variants. Full-injury models simulated the ligaments as completely ruptured, while partial injuries utilized the damaged ligamentous stiffnesses and initial toe lengths obtained from the physical experiments. Six variants of the FE model were created and analyzed with injuries at the C5–C6 level: 1) partial FC and ALL injury; 2) full FC and ALL injury; 3) partial LF and full ISL injury; 4) full LF and ISL injury; 5) partial FC, ALL, LF, and full ISL injury; and 6) full FC, ALL, LF, and ISL injury. The stiffnesses and toe lengths of the ALL and LF in the partial-injury models were adjusted to reflect the percentage stiffness reductions and initial toe length increases that were measured experimentally from the injured ligaments. Fully-injured ligaments were simulated by specifying zero stiffness to the representative computational elements. All injured ligaments were specified with zero preload force. To fit whiplash-type injury pathology, the FC ligaments were assumed to have undergone similar injury to the ALL ligaments, with stiffness values and initial toe region lengths adjusted by the same percentage as the ALL (Yang et al., 1998; Panjabi et al., 2004; Tominaga et al., 2006; Zhang et al., 2008). For the hyperflexion-type injuries, reports of whiplash pathology have shown that the ISL is often completely compromised (Panjabi et al., 2004). Accordingly, the elements representing the ISL were given zero stiffness in conjunction with partial LF injury. Applied loads were reduced to ±0.75 Nm because a series of pilot experiments performed by our group indicated that the compliance of the ligamentously-injured spine provides similar ROM to the intact case under these reduced moments. Furthermore, previous experimental studies have found that the severely injured spine is incapable of supporting 2 Nm moments without suffering catastrophic tissue failure (Panjabi et al., 1975).

Kinematic Experimentation

In order to validate the model predictions for ligamentous injury, the cadaveric validation tests were re-performed with the addition of scalpel-sectioning to the ligaments of interest (Figure 2). Prior to the physical ligamentous injury simulations, five of the whole (C0–C7) spines were loaded under 0.75 Nm pure moments using the same procedure as the intact model validation protocol. Vertebral ROM was recorded using identical stereophotogrammetric methods (Womack et al., 2011). Two cases were simulated via scalpel-sectioning at the C5–C6 level for each spine in the following order: 1) full FC and

ALL injury; and 2) full FC, ALL, LF, and ISL injury, with the testing regimen repeated after each simulated injury.

Results

The ligamentous injury data indicate a significant (p<0.0001), permanent increase in initial toe length after damage for all specimens (average increases of 1.87 mm = 524% for ALL, 2.82 mm = 302% for LF; Table 1; Figure 3). Similarly, all specimens required greater displacement to reach 40 N of force (average increases of 2.17 mm = 322% for ALL, 2.78 mm = 163% for LF). Stiffness within the 10–40 N range experienced only a minor, insignificant reduction for the LF specimens (15.3% average drop), but a much larger, significant (p<0.0001) reduction for the ALL specimens (57.6% average drop, Table 2). There was no significant difference in initial toe region length or stiffness within the two pre-damage measurement timepoints or the three post-damage measurements. The force/displacement data were highly linear within the individual force ranges, with standard Pearson's correlation coefficients (r^2) averaging 0.99 (standard deviation: 0.014) for all segments.

The average peak force for the ALL specimens during the damage step was 590 N (standard deviation: 243 N), whereas the LF specimens attained an average of 353 N (standard deviation: 149 N). The ALL ligaments extended to an average displacement of 3.57 mm (standard deviation: 0.77 mm) during the damage step. The LF specimens averaged 4.99 mm (standard deviation: 1.65 mm) of displacement during this event. Tearing damage was visible solely within the mid-substance region for all specimens; no avulsion fractures were noted. No slippage of the bony tissues was detected within the PMMA fixtures.

As a result of the extreme post-injury laxity, the ligaments provided negligible tensile support throughout physiologic spinal motion. Accordingly, FE simulations of the spinal kinematics predicted increased ROM over the intact case for each ligamentous injury (Figure 4). Minimal differences between partial and full injury ROM were predicted, with the lone exception to this finding being the extreme ligamentous injury case (FC+ALL+LF +ISL damage) during flexion and extension motion. Simulated hyperextension (FC+ALL) injuries predicted greater ROM versus hyperflexion (LF+ISL) injuries for axial rotation and lateral bending. Hyperextension injury ROM was slightly reduced (3.0% smaller) throughout flexion and extension when compared to the hyperflexion case.

Discussion

A primary goal of this research endeavor was to physically simulate whiplash-type trauma on isolated cervical ligaments. The previously-published ligamentous extensions reported during "whiplash sled"-simulated dynamic whiplash events are very similar to the data generated during the damage step of our experimentation (ALL: 3.4 mm vs 3.57 mm, LF: 4.6 mm vs 4.99 mm, for the whiplash-sled and current studies, respectively) (Ivancic et al., 2004; Panjabi et al., 2004). Thus, we conclude that the current damage protocol closely approximates the ligamentous trauma experienced by whole, osteoligamentous, cadaveric cervical spines during dynamic 8g rear and frontal whiplash-type impacts.

The cervical kinematic effects due to ligamentous hyperstrain are also similar to data that has been previously reported using whole cadaveric spines. The current hyperextension (FC and ALL partial damage) FE model predicted a 19.2% increase in C5–C6 combined flexion +extension ROM over the intact case, while the aforementioned 8g rear impact study measured a 15.9% increase at the C5–C6 level after a comparable injury (Ivancic et al., 2004). It should be noted that the referenced study applied the impact trauma to all cervical

tissues, including the intervertebral discs. In contrast, the current FE models predicted similar ROM without altering the properties of the disc. Therefore, we postulate that the damaged ligamentous tissues fail to limit motion and are primarily responsible for the resultant supra-physiologic ROM. Accordingly, these ligaments should be closely evaluated when assessing cervical stability in whiplash trauma victims.

Although the partially-damaged ligaments maintained partial component stiffness, the FE models predicted minimal difference in cervical ROM between the partially and fully-damaged spines. These models revealed that the partially-damaged ligaments generally did not extend beyond their initial toe regions during cervical motion. Thus, only trivial tensile forces were accumulated within these tissues throughout physiologic ROM, approximating the non-existent support provided by fully-damaged ligaments. The sole exception was predicted for the FC+ALL+LF+ISL case, where a lack of FC and ALL integrity permitted sufficient flexion ROM to eventually load the partially-damaged LF beyond its initial toe region.

While experimental simulation of the FC ligaments would have been ideal, the replication of the simultaneous biaxial (tangential and tensile) loading experienced by these ligaments was not possible with our current apparatus. However, substantial FC damage is nearly-universally found in severe whiplash-type hyperextension cases (Yang et al., 1998; Panjabi et al., 2004; Tominaga et al., 2006; Zhang et al., 2008). Previous experimental studies of the FC ligaments have also found a distinct discontinuity in their force/displacement curves that indicated partial damage (Winkelstein et al., 2000; Siegmund et al., 2001). This same event signaled the onset of partial damage in the current ALL and LF specimens.

Ligamentous mechanical properties demonstrated minimal variance within the two pre-damage and three post-damage measurements. However, the ligamentous stiffness and initial toe length data from the second pre-damage tensile test (Step 4 from the ligament testing procedure) are reported because they demonstrated more linearity (higher r^2 values) than data from the first pre-damage test (Step 2). This effect is likely due to the second preconditioning sequence received by the specimens prior to the later reading. The reported post-damage stiffnesses and displacements are from the 90 minute timepoint since most clinical injury analyses occur more than 90 minutes after the injury event (Marion et al., 1998). It does not appear that the ligaments demonstrate full anelasticity *in-vitro*, as an extended experimental protocol used for the initial 12 ligament specimens (6 ALL and 6 LF) also found that the mechanical properties were not significantly different between readings taken at 90 minutes, 270 minutes, and 16 hours after the simulated damage.

In conclusion, it was found that the ligaments sustain significant initial toe length distension after whiplash-type injuries. The laxity of these injured ligaments provided negligible support to the spine, resulting in nearly-identical kinematic responses to spines with no ligamentous support. Accordingly, victims of severe ligamentous hyperstrain appear to require the same degree of clinical stabilization as patients presenting fully-torn ligaments.

Acknowledgments

References

Dickerman RD, Mittler MA, Warshaw C, Epstein JA. Spinal cord injury in a 14-year-old male secondary to cervical hyperflexion with exercise. Spinal Cord. 2006; 44(3):192–195. [PubMed: 16130020]

Dickman CA, Mamourian A, Sonntag VK, Drayer BP. Magnetic resonance imaging of the transverse atlantal ligament for the evaluation of atlantoaxial instability. J Neurosurg. 1991; 75(2):221–227. [PubMed: 2072158]

Foreman, SM.; Croft, AC. Whiplash injuries : the cervical acceleration/deceleration syndrome. Philadelphia: Lippincott Williams & Wilkins; 2002.

Hogan GJ, Mirvis SE, Shanmuganathan K, Scalea TM. Exclusion of unstable cervical spine injury in obtunded patients with blunt trauma: is MR imaging needed when multi-detector row CT findings are normal? Radiology. 2005; 237(1):106–113. [PubMed: 16183927]

Ito S, Ivancic PC, Panjabi MM, Cunningham BW. Soft tissue injury threshold during simulated whiplash: a biomechanical investigation. Spine (Phila Pa 1976). 2004; 29(9):979–987. [PubMed: 15105668]

Ivancic PC, Pearson AM, Panjabi MM, Ito S. Injury of the anterior longitudinal ligament during whiplash simulation. Eur Spine J. 2004; 13(1):61–68. [PubMed: 14618382]

Lucas SR, Bass CR, Salzar RS, Oyen ML, Planchak C, Ziemba A, Shender BS, Paskoff G. Viscoelastic properties of the cervical spinal ligaments under fast strain-rate deformations. Acta Biomater. 2008; 4(1):117–125. [PubMed: 17923449]

Marion DW, Domeier R, Dunham CM, Luchette FA, Haid R, Erwood SC. PRACTICE MANAGEMENT GUIDELINES FOR IDENTIFYING CERVICAL SPINE INJURIES FOLLOWING TRAUMA. Eastern Association for the Surgery of Trauma. 1998

Mow, VC.; Huiskes, R. Basic Orthopaedic Biomechanics and Mechano-Biology: Third Edition. Philadelphia, PA: Lippincott Williams & Williams; 2005.

Panjabi MM, Maak TG, Ivancic PC, Ito S. Dynamic intervertebral foramen narrowing during simulated rear impact. Spine (Phila Pa 1976). 2006; 31(5):E128–E134. [PubMed: 16508536]

Panjabi MM, Pearson AM, Ito S, Ivancic PC, Gimenez SE, Tominaga Y. Cervical spine ligament injury during simulated frontal impact. Spine (Phila Pa 1976). 2004; 29(21):2395–2403. [PubMed: 15507801]

Panjabi MM, White AA 3rd, Johnson RM. Cervical spine mechanics as a function of transection of components. J Biomech. 1975; 8(5):327–336. [PubMed: 1184604]

Siegmund GP, Myers BS, Davis MB, Bohnet HF, Winkelstein BA. Mechanical evidence of cervical facet capsule injury during whiplash: a cadaveric study using combined shear, compression, and extension loading. Spine (Phila Pa 1976). 2001; 26(19):2095–2101. [PubMed: 11698885]

Tominaga Y, Ndu AB, Coe MP, Valenson AJ, Ivancic PC, Ito S, Rubin W, Panjabi MM. Neck ligament strength is decreased following whiplash trauma. BMC Musculoskelet Disord. 2006; 7:103. [PubMed: 17184536]

White, AA., III; Panjabi, MM. Clinical Biomechanics of the Spine: Second Edition. Philadelphia, PA: J.B. Lippincott Company; 1990.

Winkelstein BA, Nightingale RW, Richardson WJ, Myers BS. The cervical facet capsule and its role in whiplash injury: a biomechanical investigation. Spine (Phila Pa 1976). 2000; 25(10):1238–1246. [PubMed: 10806500]

Womack W, Leahy P, Patel V, Puttlitz C. Finite element modeling of kinematic and load transmission alterations due to cervical intervertebral disc replacement. Spine (Phila Pa 1976). 2011

Yang, KH.; Zhu, F.; Luan, F.; Zhao, L.; Begeman, PC. 42nd Stapp Car Crash Conference proceedings. Society of Automotive Engineers, Inc.; 1998. Development of a Finite Element Model of the Human Neck; p. 195-205.

Zhang QH, Tan SH, Teo EC. Finite element analysis of head-neck kinematics under simulated rear impact at different accelerations. Proc Inst Mech Eng H. 2008; 222(5):781–790. [PubMed: 18756695]
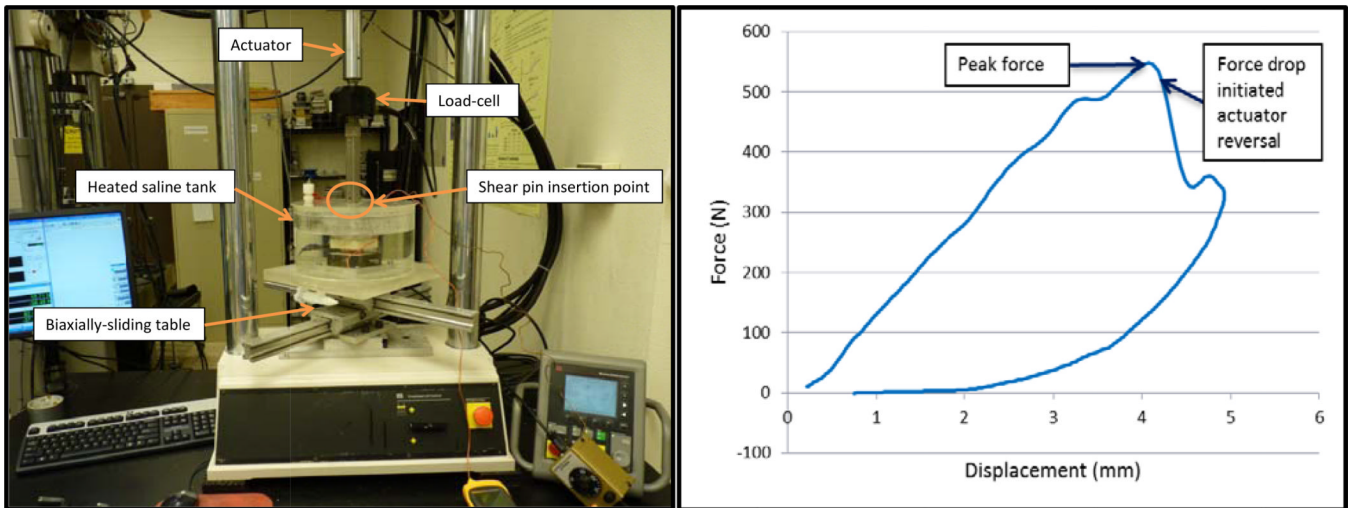
Figure 1.
(Left) The ligament tensile-testing apparatus. (Right) A typical damage step force/displacement curve at 50 mm/s loading. It can be noted that displacement continued to briefly increase after the force drop before the actuator decelerated and reversed, indicating system lag (average of 23 milliseconds).
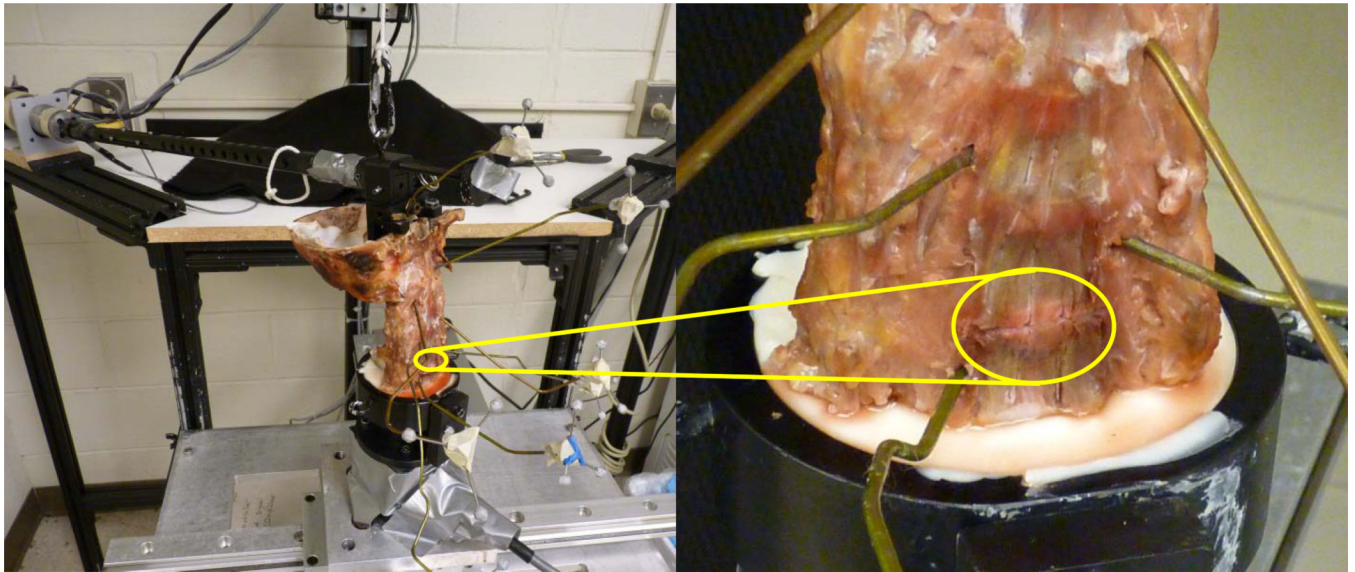
Figure 2.
(Left) Cadaveric spine in pure-moment testing apparatus. The loading arm is attached to the superior aspect of the construct while the caudal portion is fixed. Stereophotogrammetric triads for measuring ROM are shown attached to extension wires. (Right) Close-up view of a scalpel-sectioned C5–C6 ALL. Yellow circles highlight the injured tissue.
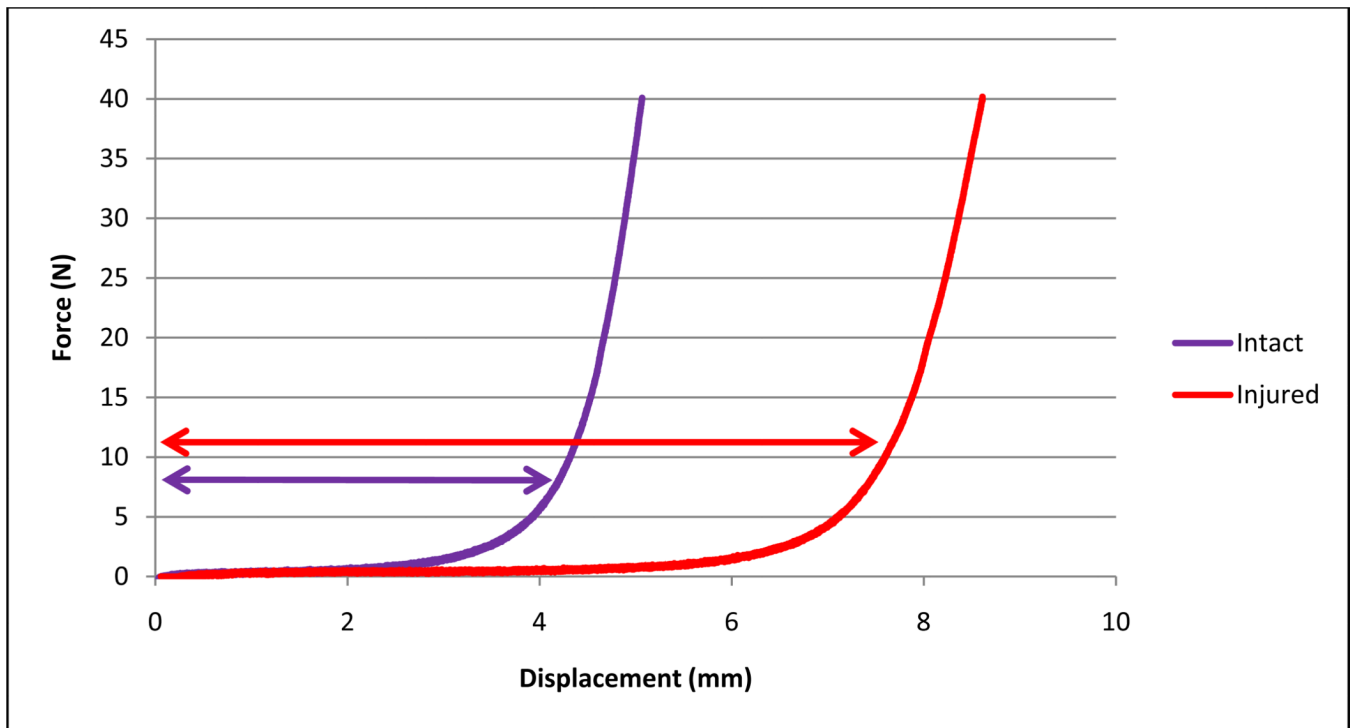
Figure 3.
A typical ligament force/displacement plot shows an increase in initial toe region length
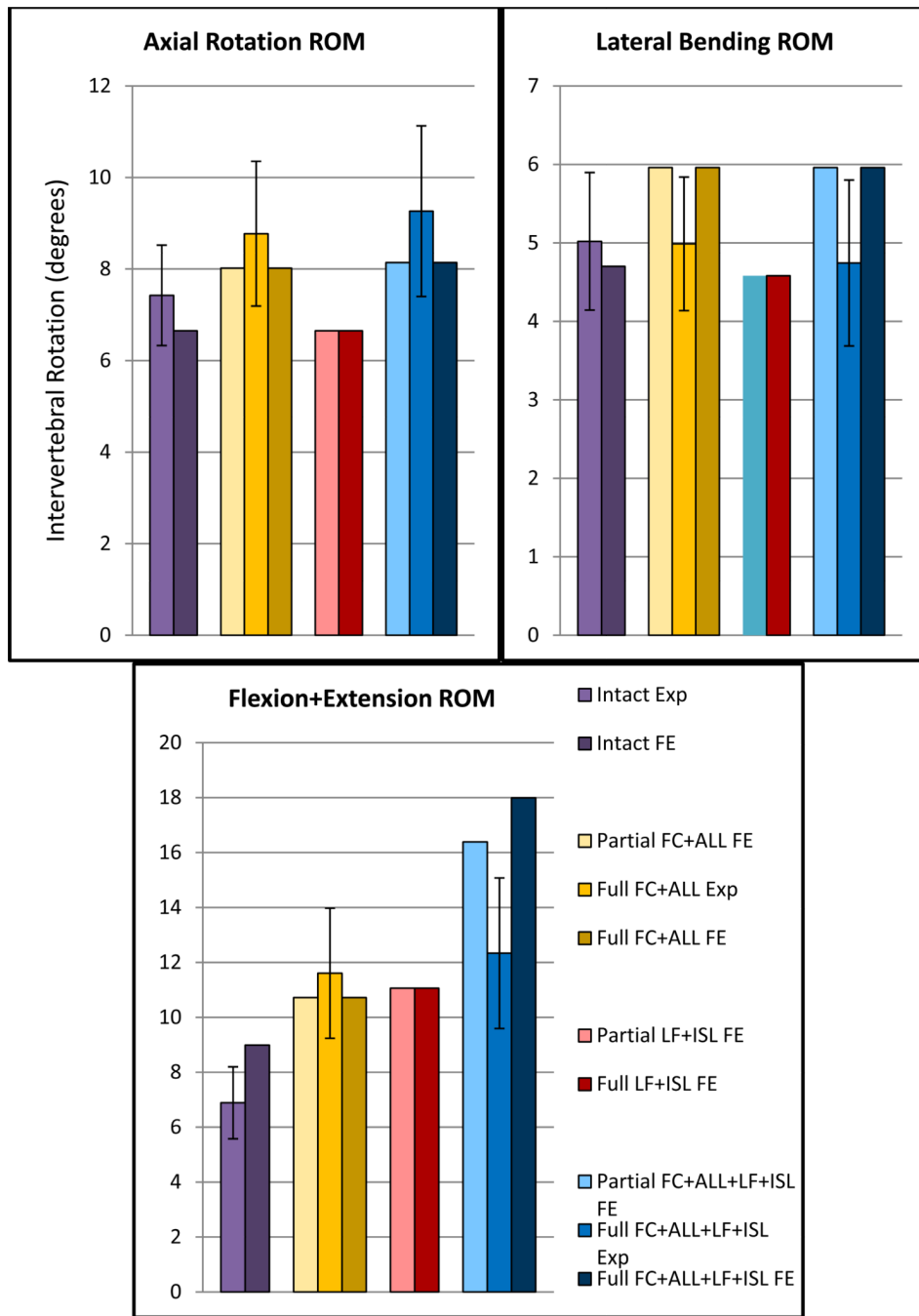(displacement at 10 N, denoted by arrows) after injury.

Figure 4.
Experimentally-measured (Exp) and finite element (FE)-predicted C5–C6 ROM for the various ligamentous injuries over ±0.75 Nm loading. Standard deviation bars are shown for experimental data.

Table 1

Ligament displacement at reference forces before and 90 minutes after induced damage. The standard deviations are shown in parentheses. Significant (p<0.01) differences are shown in shaded cells.

Type	Reference Force: N	Average Pre-Damage Displacement at Reference Force: mm	Average Post-Damage Displacement at Reference Force: mm	Average Increase in Displacement After Damage: mm	Average Percentage Increase in Displacement After Damage
ALL	10	0.51 (0.31)	2.38 (0.93)	1.87 (0.93)	524%
	40	0.85 (0.38)	3.05 (0.70)	2.17 (0.65)	322%
LF	10	1.40 (1.07)	4.22 (1.57)	2.82 (0.89)	302%
	40	2.28 (1.41)	5.16 (2.02)	2.78 (0.88)	163%

Table 2

Ligament stiffness before and 90 minutes after induced damage. The standard deviations are shown in parentheses. Significant (p<0.01) differences are shown in shaded cells.

Type	Range: N	Average Pre-Damage Stiffness: N/mm	Average Post-Damage Stiffness: N/mm	Average Stiffness Reduction: N/mm	Average Stiffness Reduction Percentage
ALL	10–20	80.73 (35.56)	29.70 (14.54)	51.03 (34.12)	59.7%
	20–30	108.70 (31.75)	43.91 (18.77)	64.79 (32.47)	57.6%
	30–40	135.59 (47.59)	60.25 (29.42)	82.43 (46.55)	55.5%
	10–40	103.34 (44.88)	43.84 (24.62)	65.27 (39.82)	57.7%
LF	10–20	36.51 (18.88)	29.18 (14.48)	7.33 (9.44)	14.5%
	20–30	57.30 (20.94)	46.59 (16.39)	10.72 (13.78)	16.2%
	30–40	76.85 (24.62)	60.80 (21.09)	14.02 (22.58)	15.3%
	10–40	55.72 (26.86)	45.09 (21.65)	10.50 (15.99)	15.3%